JOURNAL OF SOLID STATE CHEMISTRY **136,** 258–262 (1998)
ARTICLE NO. SC977697

The Aluminum-Rich Part of the System $BaO–Al_2O_3–MgO$

II: Crystal Structure of the β-Alumina-Related Compound, $Ba_2Mg_6Al_{28}O_{50}$

Nobuo Iyi,*,[1] Matthias Göbbels,† and Shigeyuki Kimura*

*National Institute for Research in Inorganic Materials, Namiki 1-1, Tsukuba-shi, Ibaraki 305, Japan; and †Institut für Kristallographie, RWTH Aachen, Jägerstrasse 17–19, 52056 Aachen, Germany

Received May 16, 1996; in revised form January 21, 1997; accepted January 22, 1997

The crystals of a new phase, $Ba_2Mg_6Al_{28}O_{50}$, recently confirmed to exist in the system $BaO–Al_2O_3–MgO$, were grown by the floating zone method, and its crystal structure was determined by using single-crystal X-ray diffraction. The space group was $P\bar{6}m2$ with lattice parameters $a = 5.638$ Å and $c = 31.983$ Å. Structure refinement revealed stacking of conduction layers of the β-alumina-type (BaO) separated by an extended spinel block ($(Al,Mg)_{17}O_{24}$). This is the same structure with Naβ'''-alumina whose ideal formula is $Na_2O \cdot 4MgO \cdot 15Al_2O_3$ ($Na_2Mg_4Al_{30}O_{50}$).

INTRODUCTION

The hexaaluminates exhibit layer structures, which consist of so-called "conduction layers" and spinel blocks stacking alternately in the *c* direction (1, 2). The difference of the conduction plane defines two major structure groups: magnetoplumbite-type and β-alumina-type (2). Modification of the conduction layer and the spinel block stacking sequence leads to further variations of the hexaaluminate structure.

β-Alumina is well known for the Na hexaaluminate (3); however, magnetoplumbite or β-alumina structures have been also known to incorporate alkaline earth elements (4–14). The structure refinements have revealed that Ca and Sr hexaaluminates were of magnetoplumbite-type (4–6) and that Ba hexaaluminates were of β-alumina-type (10–14). In the case of Ba hexaaluminates, two kinds of Ba β-alumina-type compounds were found, $Ba_{0.75}Al_{11}O_{17.25}$ and $Ba_{2.33}Al_{21.33}O_{34.33}$ (7–9), and their structures were analyzed (10–14).

The small divalent cation Mg^{2+} is not incorporated in the conduction layer but does replace Al^{3+} ions in the spinel block (15). The difference of their ionic valences causes some kind of modification in the structure. In the case of the $CaO–Al_2O_3–MgO$ system, addition of MgO does not result in a change of the magnetoplumbite-type conduction layer but in an expansion of the spinel blocks by insertion of a spinel unit ($Mg_2Al_4O_8$), as revealed in CAM-I ($Ca_2Mg_2Al_{28}O_{46}$) and CAM-II ($CaMg_2Al_{16}O_{27}$) (16, 17). In contrast, in the case of the $SrO–Al_2O_3–MgO$ system, the conduction layer is changed from magnetoplumbite-type ($SrAl_{12}O_{19}$) to β-alumina type ($SrMgAl_{10}O_{17}$, SAM-II) with an intermediate phase SAM-I ($Sr_2MgAl_{22}O_{36}$), in which two types of the conduction layers (β-alumina- and magnetoplumbite-type) stack alternately and are separated by normal spinel blocks (18). As for the $BaO–Al_2O_3–MgO$ system, three phases were reported: $BaMgAl_{10}O_{17}$, $BaMg_2Al_{14}O_{24}$, and $BaMg_3Al_{14}O_{25}$ (19, 20). So far, only the $BaMgAl_{10}O_{17}$ phase was confirmed, and its structure was determined to be of typical β-alumina-type (21). As for the other two phases, their existence has not been confirmed.

Recently, we conducted a phase study of the system $BaO–Al_2O_3–MgO$ (22, 23) and were able to confirm the presence of the $BaMg_3Al_{14}O_{25}$ ($= Ba_2Mg_6Al_{28}O_{50}$) phase but not the $BaMg_2Al_{14}O_{24}$ phase. Single-crystal growth of $Ba_2Mg_6Al_{28}O_{50}$ was attempted, and single crystals for structure determination were successfully obtained.

The details of the phase study are presented in Part I of this series (see Ref. (23)). In the present paper, the crystal structure of the new phase $Ba_2Mg_6Al_{28}O_{50}$ (BAM-II) is reported.

EXPERIMENTAL

Crystal Growth

High-purity reagents $BaCO_3$, MgO, and Al_2O_3 (99.9% Kojyundo Co.) were mixed in stoichiometric ratios under acetone in an agate mortar. After calcination of the homogenized batches at 1100°C, the powder was hydrostatically pressed to give rods of suitable size. The sintering was conducted in a molybdenum-wound resistance furnace at

[1]To whom correspondence should be addressed.

0022-4596/98 $25.00

1700°C under an oxygen atmosphere. For crystal growth, an infrared radiation convergence type FZ apparatus (24; Nichiden Machinery Ltd., NEC) equipped with a xenon lamp as the heat source was used. The growth rate was 2 mm/h in air. The resulting crystals were compositionally analyzed by EPMA (electron probe microanalyzer, JEOL JXA-8600) and used for the X-ray diffraction study.

X-Ray Data Collection

Several crystal cubes were cut from the obtained boule, and they were ground to spheres. Their crystallinity and symmetry were checked by X-ray photographic methods. A sphere with radius of about 110 μm was selected for further analysis by single-crystal X-ray diffraction. Precession and Weissenberg photographs revealed that BAM-II belonged to the hexagonal crystal system. On the basis of the existence of the reflections with $l = 2n + 1$ for hhl as well the absence of superstructure reflections, the space group $P\bar{6}m2$ was assigned. The specimen was mounted on an automatic four-circle diffractometer (Enraf-Nonius, CAD-4), and the intensities were measured using graphite-monochromatized MoKα radiation ($\lambda = 0.71068$ Å) in the 2θ–ω scanning mode up to $2\theta = 80°$. Reflections with $h \geq 0$, $k \geq 0$, $57 \geq l \geq -57$ together with their Friedel pairs. Lorenz and polarization corrections were applied. The absorption due to the crystal shape was corrected (25) by using a linear absorption coefficient (33.95 cm^{-1}). A set of four standard reflections was used to monitor the data acquisition procedure. Merging the intensities from four sets of symmetry-equivalent reflections and omission of the reflections with $I < 3\sigma(I)$ gave a total of 705 nonzero independent reflections. The larger of two types of $\sigma(F)$ for each reflection, i.e. the $\sigma(F)$ based on the counting statistics or the $\sigma(F)$ calculated by the averaging of the equivalent reflections, was used as the weighing factor in the least-squares refinement ($w = 1/\sigma(F)^2$). The weighted agreement factor among equivalent reflections was $wR = \sum w|F - F_{average}|/\sum w|F| = 0.042$.

Refinement

The full-matrix least-squares refinement was conducted by using the modified version of RSFLS-4 program (26) with neutral scattering factors (27). The Fourier syntheses were done using RSSFR-5 (28). Anomalous dispersion effects of Ba and Al were taken into account.

The lattice parameters of both compounds were also determined on the basis of 2θ data (20 reflections with a 2θ range of 55–65°, MoKα_1 radiation, $\lambda = 0.70926$ Å) collected on the four-circle diffractometer. Error values in parentheses with no decimal point correspond to the least significant digit in the function values.

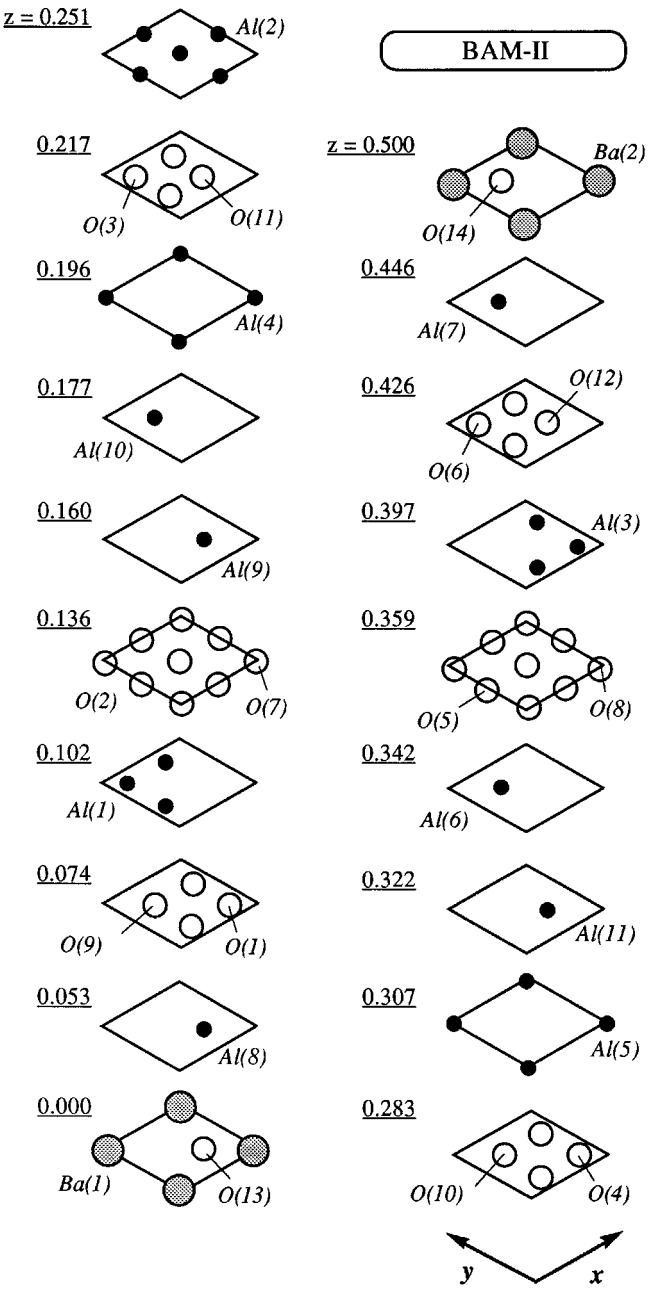

FIG. 1. The structure of BAM, shown by section at various z-values. Large filled circles represent the large cations (Ba^{2+}), small filled circles are Al ions, and large open circles are oxygen atoms.

RESULTS AND DISCUSSION

The final anisotropic refinement converged successfully to yield $R = \sum||F_o| - |F_c||/\sum|F_o| = 0.048$ ($wR = (\sum w(|F_o| - |F_c|)^2/\sum w|F_o|^2)^{1/2} = 0.063$, $S = [\sum w(|F_o| - |F_c|)^2/(m-n)]^{1/2} = 1.33$) . The polarity due to the anomalous dispersion of Ba and Al was examined by refining the model with all hkl's replaced with the Friedel pairies $\bar{h}\bar{k}\bar{l}$'s. The ratio of

TABLE 1
Crystallographic Data for BAM-II

Symmetry	Hexagonal
Space group	$P\bar{6}m2$
Cell const.	$a = 5.638(2)$ Å
	$c = 31.983(5)$ Å
	$V = 880.4(3)$ Å^3
	$z = 1$
Formula[a]	$Ba_{1.84(4)}Mg_{5.0(2)}Al_{28.8(2)}O_{50}$
Formula (ideal)	$Ba_2Mg_6Al_{28}O_{50}$

[a] Experimental value, determined by EPMA.

$wR(\bar{h}\,\bar{k}\,\bar{l})/wR(hkl)$ was found to be 1.08. Maximum residual electron densities in the final difference Fourier maps were $+7.0$e/Å^3 at (0, 0, 0.5) and -4.5e/Å^3 at (0, 0, 0.47). No secondary extinction effect was observed. The crystallographic data are listed in Table 1, and their positional parameters, bond lengths, and angles are listed in Tables 2, 3, and 4, respectively.

The refinement revealed that the structure of BAM-II is an alternate stacking of β-alumina type conduction layers and elongated spinel blocks in the c direction. This structure is the same as the so-called Na β'''-alumina ideally expressed as $Na_2Mg_4Al_{30}O_{50}$ (29, 30), which has a narrow compositional area in the Na_2O–Al_2O_3–MgO system. A similar structure was also found in a CaMg hexaaluminate by the present authors (16, 17) but with the conduction plane of the magenetoplumbite type.

Replacement of trivalent Al^{3+} ions in the spinel block by Mg^{2+} causes a necessary modification in the structure due to the difference of their ionic valences. In the previous paper (18), we pointed out two types of possibilities to incorporate Mg in these hexaaluminate structures containing divalent Ca, Sr, or Ba cations.

Type I. Mg replaces Al in the spinel block with modification of the conduction layer, changing the defect or conduction layer type (magnetoplumbite or β-alumina) and thus attaining a charge compensation.

TABLE 2
Positional and Thermal Parameters of BAM-II

Atom	Site	Number per unit cell	Positional parameters[a]		Thermal parameters[b] ($\times 10^4$)				
			x	z	U_{11}	U_{33}	U_{12}	U_{13}	B_{eq}[c]
Ba(1)	3j	0.87(1)	0.010(5)	0	288(103)	42(22)	224(115)	0	1.35(77)
Ba(2)	1b	1	0	1/2	171(10)	131(25)	$0.5U_{11}$	0	1.24(9)
Al(1)	6n	6	0.1652(15)	0.1019(4)	205(28)	196(36)	113(43)	36(22)	1.56(30)
Al(2)	6n	5.73(4)	0.4984(18)	0.2505(6)	74(12)	58(12)	29(18)	23(18)	0.57(15)
Al(3)	6n	6	0.8320(9)	0.3972(3)					0.178(3)
Al(4)	2g	2	0	0.1956(7)	93(30)	90(45)	$0.5U_{11}$	0	0.73(20)
Al(5)	2g	1.74(5)	0	0.3072(8)	56(29)	78(47)	$0.5U_{11}$	0	0.50(20)
Al(6)	2h	2	1/3	0.3417(6)					1.00(9)
Al(7)	2h	2	1/3	0.4460(4)					0.111(5)
Al(8)	2i	2	2/3	0.0525(5)	270(29)	94(54)	$0.5U_{11}$	0	1.67(22)
Al(9)	2i	1.77(5)	2/3	0.1600(6)					0.372(7)
Al(10)	2h	2	1/3	0.1768(6)	92(20)	341(75)	$0.5U_{11}$	0	1.38(23)
Al(11)	2i	2	2/3	0.3215(4)					0.03(1)
O(1)	6n	6	0.8396(17)	0.0718(8)					0.88(1)
O(2)	6n	6	0.4897(19)	0.1400(7)					0.55(1)
O(3)	6n	6	0.1777(16)	0.2150(7)					0.60(1)
O(4)	6n	6	0.8132(17)	0.2832(7)					0.85(1)
O(5)	6n	6	0.5166(19)	0.3564(7)					0.78(1)
O(6)	6n	6	0.1652(19)	0.4276(8)					0.57(1)
O(7)	2g	2	0	0.1318(8)					0.14(1)
O(8)	2g	2	0	0.3621(9)					0.64(2)
O(9)	2h	2	1/3	0.0758(12)					0.92(2)
O(10)	2h	2	1/3	0.2839(9)					0.24(1)
O(11)	2i	2	2/3	0.2194(10)					1.23(2)
O(12)	2i	2	2/3	0.4241(11)					0.35(2)
O(13)	1e	1	2/3	0					0.55(3)
O(14)	1d	1	1/3	1/2					0.86(3)

[a] $y = 2x$, [b] $U_{22} = U_{11}$, $U_{23} = -U_{13}$. The thermal temperature factor is expressed as $\exp(-2\pi^2(h^2a^{*2}U_{11} + k^2b^{*2}U_{22} + l^2c^{*2}U_{33} + 2hka^*b^*U_{12} + 2hla^*c^*U_{13} + 2klb^*c^*U_{23})$. [c] $B_{eq} = \frac{4}{3}(\sum_i \sum_j B_{ij}\mathbf{a}_i\mathbf{a}_j) = \frac{8}{3}\pi^2(\sum_i \sum_j U_{ij})$.

TABLE 3
Interatomic Distances of BAM-II

	No. of bonds	Distance (Å)
	Octahedral Coordination	
Al(1)–O(1)	2	1.858(17)
–O(7)	1	1.876(14)
–O(9)	1	1.842(18)
–O(2)	2	2.002(17)
Al(2)–O(3)	2	1.936(19)
–O(10)	1	1.935(18)
–O(4)	2	1.868(18)
–O(11)	1	1.920(19)
Al(3)–O(6)	2	1.896(16)
–O(8)	1	1.989(17)
–O(12)	1	1.829(16)
–O(5)	2	2.024(16)
Al(10)–O(2)	3	1.927(17)
–O(3)	3	1.951(19)
Al(11)–O(5)	3	1.841(15)
–O(4)	3	1.885(16)
	Tetrahedral Coordination	
Al(4)–O(7)	1	2.038(34)
–O(3)	3	1.843(11)
Al(5)–O(4)	3	1.980(13)
–O(8)	1	1.757(38)
Al(6)–O(5)	3	1.850(7)
–O(10)	1	1.848(33)
Al(7)–O(6)	3	1.744(10)
–O(14)	1	1.727(12)
Al(8)–O(1)	3	1.799(11)
–O(13)	1	1.678(16)
Al(9)–O(2)	3	1.843(10)
–O(11)	1	1.901(37)
	Polyhedron 9-Coordinated	
Ba(1)–O(1)	3	2.838(21)
–O(1)′	3	2.754(26)
–O(13)	2	3.207(25)
–O(13)′	1	3.356(2)
Ba(2)–O(6)	6	2.822(21)
–O(14)	3	3.256(2)

TABLE 4
Interatomic Angles of BAM-II

	No. of bonds	Angle (deg)
	Octahedral Coordination	
O(1)–Al(1)–O(1)′	1	93.82(93)
O(1)–Al(1)–O(2)	2	91.64(65)
O(1)–Al(1)–O(9)	2	99.45(95)
O(1)–Al(1)–O(7)	2	83.09(69)
O(2)–Al(1)–O(2)′	1	82.67(68)
O(2)–Al(1)–O(7)	2	93.81(74)
O(2)–Al(1)–O(9)	2	83.37(89)
O(3)–Al(2)–O(3)′	1	85.69(89)
O(3)–Al(2)–O(4)	2	95.49(66)
O(3)–Al(2)–O(10)	2	87.57(66)
O(3)–Al(2)–O(11)	2	94.21(95)
O(4)–Al(2)–O(4)′	1	83.12(83)
O(4)–Al(2)–O(10)	2	96.01(93)
O(4)–Al(2)–O(11)	2	82.18(75)
O(5)–Al(3)–O(5)′	1	77.70(63)
O(5)–Al(3)–O(6)	2	93.45(58)
O(5)–Al(3)–O(8)	2	89.72(70)
O(5)–Al(3)–O(12)	2	85.32(79)
O(6)–Al(3)–O(6)′	1	94.99(88)
O(6)–Al(3)–O(8)	2	85.78(68)
O(6)–Al(3)–O(12)	2	98.49(81)
O(2)–Al(10)–O(2)′	3	86.70(94)
O(2)–Al(10)–O(3)	6	94.18(58)
O(3)–Al(10)–O(3)′	3	84.92(98)
O(4)–Al(11)–O(4)′	3	82.19(84)
O(4)–Al(11)–O(5)	6	95.26(59)
O(5)–Al(11)–O(5)′	3	87.20(84)
	Tetrahedral Coordination	
O(3)–Al(4)–O(3)′	3	109.26(91)
O(3)–Al(4)–O(7)	3	109.68(90)
O(4)–Al(5)–O(4) ′	3	105.94(97)
O(4)–Al(5)–O(8)	3	112.81(87)
O(5)–Al(6)–O(5)′	3	113.83(66)
O(5)–Al(6)–O(10)	3	104.66(83)
O(6)–Al(7)–O(6)′	3	109.25(85)
O(6)–Al(7)–O(14)	3	109.69(85)
O(1)–Al(18)–O(1)′	3	108.80(91)
O(1)–Al(18)–O(13)	3	110.13(88)
O(2)–Al(9)–O(2)′	3	108.66(82)
O(2)–Al(9)–O(11)	3	110.27(80)

Type II. A spinel unit ($Mg_{2-x}Al_{4+x}O_8$) is inserted in the Al–spinel blocks, forming extended spinel blocks and thus attaining the charge compensation.

In the case of the compounds CAM-I ($Ca_2Mg_2Al_{28}O_{46}$) and CAM-II ($CaMg_2Al_{16}O_{27}$), type II compensation occurs without changing the magenetoplumbite-type conduction layer. In the case of Sr hexaaluminates, $SrAl_{12}O_{19}$ is known to have magenetoplumbite structure (6); in SAM-I, half of the conduction layer is changed to β-alumina-type, and for SAM-II, all conduction layers were of β-alumina type, where extended spinel blocks were not observed (18). In the case of BaMg hexaaluminates, $Ba_{0.75}Al_{11}O_{17.25}$ is of β-alumina-type with some defects at the Ba site and others (13, 14). The type I mechanism of Mg incorporation finally takes place to form $BaMgAl_{10}O_{17}$, where the defect in the conduction layer has vanished (21). The difference is only the defect structure in the conduction layer. The basic β-alumina-type conduction layer is maintained. For further

incorporation of MgO, a type II mechanism occurs, leading to the ideal composition of $Ba_2Mg_6Al_{28}O_{50}$.

Pinpointing the Mg substitution site is difficult by the X-ray method, but, judging from the average bond lengths of Al(5) and Al(4) tetrahedra (Al(5)–O, 1.92 Å; Al(4)–O, 1.89 Å), Mg would be highly concentrated at the Al(5) and Al(4) sites. The assumption is based on the fact that Mg incorporation at the Al site enlarges the bond length. In the case of MgO-containing Na β'''-alumina, the average Al–O bond length of the corresponding tetrahedral Al site (the 4e site) is 1.77 Å (29). The average bond lengths of Al(6) and Al(9) tetrahedra (Al(6)–O, 1.85 Å; Al(9)–O, 1.86 Å) are also larger than that of the corresponding Al site (4f with $z = 0.0701$) in the MgO-containing Na β'''-alumina (29). This indicates the partial occupancy of Mg at these sites. It is reasonable because the Mg content of BAM-II (5.0 ± 0.2 per unit cell) is greater than the number available by the Al(5) and Al(4) sites (4 per unit cell).

The result of EPMA shows that the crystal obtained is shifted to the Al-rich side in the solid solution range with a small amount of Ba defects. To reveal the defect site distribution in this structure, the occupancy was refined further. The occupancy factors of Ba sites were further varied in the least-square refinement. The result showed the alternate Ba occupancy in the conduction planes. This means that there are two types of the conduction plane: Ba vacancy containing conduction layer and fully occupied conduction layer. BAM-II has the same structure with Na β'''-alumina ($Na_2O \cdot 4MgO \cdot 15Al_2O_3$), but the Na β'''-alumina has the higher symmetric space group $P6_3/mmc$. The Ba vacancy as well as uneven distribution of Mg in the spinel block would have made the space group $P\bar{6}m2$.

ACKNOWLEDGMENTS

The authors are very grateful to Mr. S. Takekawa (NIRIM) for his advice for the crystal growth and to Mr. K. Kosuda (NIRIM) for help in electron probe microanalysis. This study was performed through Special Coordination Funds of the Japanese Science and Technology Agency, to whom we are deeply indebted.

REFERENCES

1. J. T. Kummer, "Progress in Solid State Chemistry," Vol. 7, p. 141. Pergamon Press, Oxford, 1972.
2. N. Iyi, S. Takekawa, and S. Kimura, *J. Solid State Chem.* **83,** 8 (1989).
3. C. R. Peters, M. Bettman, J. W. Moore, and D. Glick, *Acta Crystallogr. Sect. B* **27,** 1826 (1971).
4. K. Kato and H. Saalfeld, *N. Jb. Miner. Abh.* **109,** 192 (1968).
5. A. Utsunomiya, K. Tanaka, H. Morikawa, F. Marumo, and H. Kojima, *J. Solid State Chem.* **75,** 197 (1988).
6. A. J. Lindop, C. Matthews, and D. W. Goodwin, *Acta Crystallogr. Sect. B* **31,** 2940 (1975).
7. F. Haberey, G. Oehlschlegel, and K. Sahl, *Ber. Dt. Keram. Ges.* **54,** 373 (1977).
8. S. Kimura, E. Bannai, and I. Shindo, *Mater. Res. Bull.* **17,** 209 (1982).
9. N. Iyi, S. Takekawa, Y. Bando, and S. Kimura, *J. Solid State Chem.* **47,** 34 (1983).
10. N. Iyi, Z. Inoue, S. Takekawa, and S. Kimura, *J. Solid State Chem.* **52,** 66 (1984).
11. N. Iyi, Z. Inoue, S. Takekawa, and S. Kimura, *J. Solid State Chem.* **60,** 41 (1985).
12. N. Iyi, Y. Bando, S. Takekawa, and Y. Kitami, *J. Solid State Chem.* **64,** 220 (1986).
13. N. Iyi, S. Takekawa, and S. Kimura, *J. Solid State Chem.* **59,** 250 (1985).
14. F. P. F. van Berkel, H. W. Zandbergen, G. C. Vershoor, and D. J. W. Ijdo, *Acta Crystallogr. Sect. C* **40,** 1124 (1984).
15. W. L. Roth, F. Reidinger, and S. LaPlaca, *in* "Superionic Conductors" (G. D. Mahan and W. L. Roth, Eds.), p. 223. Plenum, New York, 1977.
16. M. Göbbels, E. Woermann, and J. Jung, *J. Solid State Chem.* **120,** 358 (1995).
17. N. Iyi, M. Göbbels, and Y. Matsui, *J. Solid State Chem.* **120,** 364 (1995).
18. N. Iyi and M. Göbbels, *J. Solid State Chem.* **122,** 46 (1996).
19. J. M. P. J. Verstegen and A. L. N. Stevels, *J. Lumin.* **9,** 406 (1974).
20. A. L. N. Stevels and A. D. M. Schrama-de Pauw, *J. Electrochem. Soc.* **123,** 691 (1976).
21. N. Iyi, Z. Inoue, and S. Kimura, *J. Solid State Chem.* **61,** 236 (1986).
22. S. Kimura, NIRIM REPORT (1983).
23. M. Göbbels, S. Kimura, and E. Woermann, *J. Solid State Chem.* **136,** 253 (1998).
24. S. Kimura and I. Shindo, *J. Cryst. Growth.* **41,** 192 (1977).
25. W. R. Busing and H. A. Levy, *Acta Crystallogr.* **10,** 180 (1957).
26. T. Sakurai, K. Nakatsu, H. Iwasaki, and M. Fukuhara, "RSFLS-4, UNICS II." The Crystallographic Society of Japan, 1967.
27. J. A. Ibers and W. C. Hamilton, "International Tables for X-ray Crystallography," Vol. 4. Kynoch Press, Birmingham, UK, 1974.
28. T. Sakurai, "RSSFR-5, UNICS II." The Crystallographic Society of Japan, 1967.
29. M. Bettmann and L. Terner, *Inorg. Chem.* **10**, 1442 (1971).
30. Y. Matsui, Y. Bando, Y. Kitami, and J. L. Hutchison, *J. Electron Microsc.* **35,** 395 (1986).